
Defense against Privacy Leakage in Federated Learning

Jing Wu¹ Munawar Hayat² Mingyi Zhou³ Mehrtash Harandi¹

¹Department of Electrical and Computer Systems Engineering

²Department of Data Science and AI

³Department of Software Systems and Cybersecurity

{jing.wu1, munawar.hayat, mingyi.zhou, mehrtash.harandi}@monash.edu

Abstract

Federated Learning (FL) provides a promising distributed learning paradigm, since it seeks to protect users privacy by not sharing their private training data. Recent research has demonstrated, however, that FL is susceptible to model inversion attacks, which can reconstruct users' private data by eavesdropping on shared gradients. Existing defense solutions cannot survive stronger attacks and exhibit a poor trade-off between privacy and performance. In this paper, we present a straightforward yet effective defense strategy based on obfuscating the gradients of sensitive data with concealing data. Specifically, we alter a few samples within a mini batch to mimic the sensitive data at the gradient levels. Using a gradient projection technique, our method seeks to obscure sensitive data without sacrificing FL performance. Our extensive evaluations demonstrate that, compared to other defenses, our technique offers the highest level of protection while preserving FL performance. Our source code is located in the repository.

1 Introduction

We propose to conceal sensitive information via learning concealing examples as a defence strategy for Federated Learning (FL) (Konečný *et al.*, 2015). Federated Learning (FL) is a distributed learning paradigm that enables several clients (*e.g.*, mobile devices or businesses) to train a unified model jointly under the orchestration of a central server, while training data is decentralised. One of the key benefits of the FL model is that it can afford some privacy. In FL, raw user input is never transferred out of the device, and only model updates (*e.g.*, gradients) are communicated to the central server. The model updates are more focused on the learning task, hence it was thought that they could never contain more information about the training data than themselves (Kairouz *et al.*, 2021). The technology is essential for critical applications *e.g.*, learning from patients medical records across hospitals (Brisimi *et al.*, 2018), where the confidentiality of patients sensitive data is important.

Recent *model inversion attacks* (Zhu *et al.*, 2019; Geiping *et al.*, 2020; Balunović *et al.*, 2021; Fowl *et al.*, 2021) have shown, however, users' private data can be reconstructed from the shared gradients. To address the privacy leakage caused by the shared gradients, several defence ideas are explored (*e.g.*, Differential Privacy (DP) (adding noise to gradients) (Geyer *et al.*, 2017), compression (pruning gradients) (Lin *et al.*, 2017)). Unfortunately, aforementioned defences suffer from noticeable performance degradation as shown for example in (Zhu *et al.*, 2019; Sun *et al.*, 2021). Latest techniques such as Automatic Transformation Search (ATS) (Gao *et al.*, 2021) (augmenting data to hide sensitive information), PRivacy Enhancing mODule (PRECODE) (Scheliga *et al.*, 2022) (use of bottleneck to hide the sensitive data), and Soteria (Sun *et al.*, 2021) (pruning gradients in a single layer) are shown to maintain the FL performance while simultaneously preserving the privacy. Having said that, as defence techniques improve, attacks evolve as well. Recent studies such as

Balunović *et al.* (2021) raise the alarm by providing strong evidences that modern defences are not effective against stronger attacks.

To design a more competent defence and in contrast to previous defence approaches, we first argue that preserving the privacy of sensitive samples (*e.g.*, personal data revealing racial or ethnic origin, political opinions, religious beliefs, and the processing of data concerning health ¹) should be the priority of the algorithm. To ensure that the adversary is unable to reconstruct sensitive samples, while simultaneously maintaining the performance of the FL system, we propose to hide the sensitive information by learning concealing points. Specifically, we generate concealing points with high gradient similarity with the sensitive data, while reducing their visual similarity with the sensitive data. Our proposed defence has two main characteristics. **1) Enhancing the privacy of the sensitive data.** Even though the gradients from the concealing data are similar to that of the sensitive data, inverting these gradients results in data points that are visually very different than the sensitive data. This is because the gradients from the sensitive data are obfuscated with the gradients of the concealing data, thereby the reconstruction of the sensitive samples will be obfuscated with the concealing samples. As such, our proposed approach improves the privacy of sensitive data in FL. **2) Maintaining the FL performance.** Introducing concealing data can potentially harm the learning as it alters the gradient information. Our algorithm ensures that the gradient after introducing the concealing samples is still aligned with that of training samples (including sensitive data), and thus maintains the learning capabilities of the FL. To achieve our goals, we formulate the problem as an optimization problem with linear constraints.

Our main contributions can be summarized as: **1.** The proposed defence craft concealing samples which are adaptively learned to ensure privacy while simultaneously avoiding performance degradation. **2.** Our algorithm can be further combined with existing defences (*e.g.*, differential privacy) for achieving desirable privacy-performance trade-off and overheads. **3.** We thoroughly evaluate and compare our proposed algorithm against various baselines (*e.g.*, gradient compression), and empirically observe that our algorithm consistently outperform state-of-the-art methods.

2 Related work

To contextualize our contributions, we briefly review existing proposals for privacy leakage and privacy preserving methods in Federated Learning (FL).

2.1 Model Inversion Attacks

Numerous model inversion attacks to breach FL privacy have been proposed (*e.g.*, (Phong *et al.*, 2017; Fan *et al.*, 2020; Zhu *et al.*, 2019; Yin *et al.*, 2021; Jeon *et al.*, 2021). Deep Leakage from Gradients (DLG) (Zhu *et al.*, 2019) and its variants (Zhao *et al.*, 2020) (recover the target label so only optimize over the input) employ an optimization-based technique to reconstruct private data from the given gradient updates:

$$(\mathbf{x}^*, \mathbf{y}^*) = \arg \min_{(\hat{\mathbf{x}}, \hat{\mathbf{y}})} \|\nabla \mathcal{L}(f(\mathbf{x}), \mathbf{y}) - \nabla \mathcal{L}(f(\hat{\mathbf{x}}), \hat{\mathbf{y}})\|. \quad (1)$$

Here the inputs $\mathbf{x}^*, \mathbf{x}, \hat{\mathbf{x}}$ represent the reconstructed, original and randomly initialized input, respectively, while the labels $\mathbf{y}^*, \mathbf{y}, \hat{\mathbf{y}}$ are the reconstructed, original and randomly initialized label, respectively. Typically, the loss function \mathcal{L} denotes the cross-entropy loss and $f : \mathbf{x} \rightarrow \mathbf{y}$ be the model classifying the input to a label. While the original algorithm works best if the number of training samples in each batch is small, follow-up attacks (Geiping *et al.*, 2020; Wei *et al.*, 2020; Mo *et al.*, 2021; Jeon *et al.*, 2021; Yin *et al.*, 2021) such as Gradient Similarity (GS) (Geiping *et al.*, 2020) and GradInversion attack (Yin *et al.*, 2021) remove such necessities while being able to reconstruct high resolution images with larger batch sizes by using cosine similarity as the distance metric and incorporating stronger image priors. Jin *et al.* (2021) introduce catastrophic data leakage (CAFE) in vertical federated learning (VFL) and they can improve the data recovery quality over a large batch in VFL. Balunović *et al.* (2021) firstly formalize the gradient leakage problem within the Bayesian framework, and then demonstrate existing optimization-based attacks could be approximated as the optimal adversary with different assumptions on the input and gradients. In addition, they provide evidences that most existing defences are not quite effective against stronger attacks.

¹European Union’s General Data Protection Regulation

While above mentioned attacks assume the server is honest-but-curious (Goldreich, 2009), Fowl *et al.* (2021) and Boenisch *et al.* (2021) introduce model modification attacks by a malicious server. Boenisch *et al.* (2021) apply their trap weights to initialize the model with the goal of activating each neuron with a single data point, enabling millisecond-perfect reconstruction. Similarly, Fowl *et al.* (2021) propose the Imprint attack by inserting the imprint module with specific weights into the structure, allowing portions of the updates to only contain information of a subset data points, which could recover data precisely and quickly, even if the data is aggregated over large batches. Further, they introduce an imprint variant that generates sparse gradients in the case of multiple local updates.

2.2 Privacy Preserving Defences

As attacks on FL that violate users’ privacy have increased, numerous defences have been proposed. We can broadly categorize the existing defences against model inversion attacks in FL into four categories: gradient compression (Lin *et al.*, 2017; Sun *et al.*, 2021) and perturbation (Geyer *et al.*, 2017; McMahan *et al.*, 2017b), data encryption (Gao *et al.*, 2021; Huang *et al.*, 2020), architectural modifications (Scheliga *et al.*, 2022), and secure aggregation via changing the communication and training protocol (Bonawitz *et al.*, 2017; Mohassel and Zhang, 2017; Lee *et al.*, 2021; Wei *et al.*, 2021). Zhu *et al.* (2019) show that gradient compression can help, while Sun *et al.* (2021) propose Soteria, which shows gradient pruning in a single layer as a defence strategy. Differential Privacy (DP) (Geyer *et al.*, 2017; McMahan *et al.*, 2017b) adds Gaussian or Laplacian noise into the gradients, and has been shown as an effective privacy-preserving strategy in FL. Gao *et al.* (2021) introduce Automatic Transformation Search (ATS) to generate heavily augmented images for training to hide information of the sensitive data, while Huang *et al.* (2020, 2021) propose InstaHide to encrypt the private data with data from public datasets. Scheliga *et al.* (2022) introduce a PRivacy Enhancing mODule (PRECODE), which insert a VAE to hide the users’ data.

However, the study (Zhu *et al.*, 2019; Gao *et al.*, 2021; Sun *et al.*, 2021) show that DP-based defences require a large number of participants in the training process to converge and achieve a desirable privacy-performance tradeoff. Balunović *et al.* (2021) show that the adversary can drop the gradients pruned by the defence Soteria while still get an almost perfect reconstruction, even when the adversary has no idea about which layer is pruned. Balunović *et al.* (2021) also show it is easy to reconstruct the data using the GS attack in the initial communication rounds against the defence ATS, while Carlini *et al.* (2020) show that they can recover private data when they know the encodings of InstaHide. For the defence PRECODE, Balunović *et al.* (2021) show that there is always at least one non-zero entry in the bias, letting the adversary perfectly reconstruct the data. Sun *et al.* (2021) show that secure aggregation will incur unneglectable computational overhead. As defensive techniques evolve, so do attacks. We show that the recently proposed Imprint attack can evade from existing defences.

We can conclude that the current defence mechanisms are not quite effective against model inversion attacks in FL. It is therefore pertinent to design an effective defence that does not sacrifice the FL performance.

3 Methodology

In this section, we provide details of our proposed defence method against model inversion attacks. We first demonstrate the scenario, introduce a basic FL framework and discuss a simple reconstruction formulation to show how model inversion attacks work based on the shared gradients, and then describe how the proposed method defends against these attacks. Throughout the paper, we represent scalars, vectors/matrices by lowercase and bold symbols, respectively (*e.g.*, a , \mathbf{a}).

3.1 Scenario

Consider an Artificial Intelligence (AI) service that aids in disease diagnosis. Multiple hospitals train models for this service in collaboration. Publishing such a service could benefit a large number of doctors and patients, but it is critical to ensure that private medical data cannot be recovered, and that the utility of the service is normal due to a misdiagnosis or underdiagnosis could be vital. We take a malignant skin lesion recognition system as an example. Skin images contain personal information needs more attention than images without private information. As such, preserving the privacy of the former should be the priority of the defences.

3.2 Federated learning

Let $f_\theta : \mathcal{X} \rightarrow \mathcal{Y}$ be the model with parameters θ , classifying the input \mathbf{x} from the input space $\mathcal{X} \subseteq \mathbb{R}^d$ to a label \mathbf{y} in the label space \mathcal{Y} . In standard federated learning, there are C clients and a central server. With the help of multiple clients that have local training data, the server wants to solve the problem in Eqn. (2),

$$\min_{\theta} \frac{1}{C} \sum_{c=1}^C \mathbb{E}_{(\mathbf{X}, \mathbf{Y}) \sim \mathcal{D}_c} [\mathcal{L}_c(\mathbf{X}, \mathbf{Y}; \theta)], \quad (2)$$

where the client c has the loss function \mathcal{L}_c . In the t -th training round, each client c will compute the gradients $\nabla_{\theta} \mathcal{L}_c(f_\theta(\mathbf{X}_c), \mathbf{Y}_c)$ over local training data, and send these to the server. The server then updates the model parameters θ^t using gradients from the selected \tilde{C} clients:

$$\theta^t = \theta^{t-1} - \frac{\eta}{\tilde{C}} \sum_{c=1}^{\tilde{C}} \nabla_{\theta^{t-1}} \mathcal{L}_c(\mathbf{X}_c, \mathbf{Y}_c; \theta^{t-1}), \quad (3)$$

where η is the learning rate. The server propagates back the updated parameters θ^t to each client, and the whole process repeats. Even though the private training data never leaves the local clients, in the following, we show how an adversary can still reconstruct the data based on the shared gradients $\nabla_{\theta} \mathcal{L}_c(f_\theta(\mathbf{X}_c), \mathbf{Y}_c)$ from client c in the t -th communication round.

3.3 Reconstruction formulation

Several studies (Geiping *et al.*, 2020; Boenisch *et al.*, 2021; Balunović *et al.*, 2021; Fowl *et al.*, 2021) show that for models with only fully connected layers, a single non-zero entry in the gradient of the loss w.r.t. the layer's output is enough to perfectly reconstructed the input \mathbf{x} . Detailed proof can be found in Geiping *et al.* (2020). Without loss of generality, we consider the case of a network having only one fully connected layer, for which the forward pass is given by $\mathbf{y} = \mathbf{W}^T \mathbf{x} + \mathbf{b}$, where \mathbf{W} is the weight and \mathbf{b} is the bias, \mathbf{x} is the input. Let \mathcal{L} denote the objective to update the parameters, then the adversary reconstructs the input \mathbf{x} by computing the gradients of the objective w.r.t. the weight and the bias:

$$\begin{aligned} \frac{\partial \mathcal{L}}{\partial \mathbf{W}_l^T} &= \frac{\partial \mathcal{L}}{\partial \mathbf{y}_l} \cdot \frac{\partial \mathbf{y}_l}{\partial \mathbf{W}_l^T} = \frac{\partial \mathcal{L}}{\partial \mathbf{y}_l} \mathbf{x}, \\ \frac{\partial \mathcal{L}}{\partial \mathbf{b}_l} &= \frac{\partial \mathcal{L}}{\partial \mathbf{y}_l} \cdot \frac{\partial \mathbf{y}_l}{\partial \mathbf{b}_l} = \frac{\partial \mathcal{L}}{\partial \mathbf{y}_l}, \end{aligned} \quad (4)$$

where \mathbf{W}_l^T denotes the l -th line of the weight matrix \mathbf{W}^T . Thus, we can get the perfect reconstruction $\mathbf{x}' = (\frac{\partial \mathcal{L}}{\partial \mathbf{b}_l})^{-1} \frac{\partial \mathcal{L}}{\partial \mathbf{W}_l^T}$ if the entry in the gradient of the loss w.r.t. the bias $\frac{\partial \mathcal{L}}{\partial \mathbf{b}_l} \neq 0$.

This individual data point leakage has further been shown is not restricted in the case where mini-batch of size $B = 1$ (Boenisch *et al.*, 2021). When the mini-batch size $B > 1$, let $\mathbf{x}^j (j \in [1, B])$ denotes the data point in the mini-batch, so the output for each input is $\mathbf{y}^j = \mathbf{W}^T \mathbf{x}^j + \mathbf{b}$, then the gradient will be

$$\begin{aligned} \frac{\partial \mathcal{L}}{\partial \mathbf{W}_l^T} &= \frac{1}{B} \sum_{j=1}^B \left(\frac{\partial \mathcal{L}}{\partial \mathbf{y}_l^j} \cdot \frac{\partial \mathbf{y}_l^j}{\partial \mathbf{W}_l^T} \right) = \frac{1}{B} \sum_{j=1}^B \frac{\partial \mathcal{L}}{\partial \mathbf{y}_l^j} \mathbf{x}^j, \\ \frac{\partial \mathcal{L}}{\partial \mathbf{b}_l} &= \frac{1}{B} \sum_{j=1}^B \left(\frac{\partial \mathcal{L}}{\partial \mathbf{y}_l^j} \cdot \frac{\partial \mathbf{y}_l^j}{\partial \mathbf{b}_l} \right) = \frac{1}{B} \sum_{j=1}^B \frac{\partial \mathcal{L}}{\partial \mathbf{y}_l^j}. \end{aligned} \quad (5)$$

This indicates that the gradient contain a linear combination of all the data point \mathbf{x}^j in the mini-batch. Boenisch *et al.* (2021) observe that except for one training data point, all mini-batch data points have zero gradients in some cases, letting the passive adversaries can get a perfect reconstruction. While optimization-based attacks seek to compute the reconstruction via minimizing the distance between the gradient of the input and that of the reconstruction, model modification attacks utilize particular parameters aiming to amplify the accidental leakage (Boenisch *et al.*, 2021): $\frac{\partial \mathcal{L}}{\partial \mathbf{W}_l^T} = \frac{1}{B} \frac{\partial \mathcal{L}}{\partial \mathbf{y}_l^*} \mathbf{x}^*$, or allow portions of the gradients to only contain information of a subset data points (Fowl *et al.*, 2021): $\frac{\partial \mathcal{L}}{\partial \mathbf{W}_l^T} - \frac{\partial \mathcal{L}}{\partial \mathbf{W}_{l+1}^T} = \frac{1}{B} \left(\frac{\partial \mathcal{L}}{\partial \mathbf{y}_l^*} - \frac{\partial \mathcal{L}}{\partial \mathbf{y}_{l+1}^*} \right) \mathbf{x}^*$.

3.4 Defence design

Our objective is to protect sensitive data without modifying any FL system settings (*e.g.*, model structure) and the sensitive data themselves, while minimizing the impact of the proposed defence on the model performance. Given that model inversion attacks in FL reconstruct the inputs using gradients, which is the weighting of all the data points \mathbf{x}^j in the mini-batch (shown in Eqn. (5)), our key insight is to insert samples (named with Concealing Samples) that can imitate the sensitive data on the gradient level in the mini-batch, while ensuring that these samples are visually dissimilar from the sensitive data. As such, the gradients over the mini-batch will confuse the adversaries by obfuscating the gradient from the sensitive data and that from the concealing samples. Specifically, in Eqn. (5), we assume that the sensitive data point \mathbf{x}^s , we aim to craft the concealing sample \mathbf{x}^r which makes $\partial\mathcal{L}/\partial\mathbf{y}_i^r$ approaching $\partial\mathcal{L}/\partial\mathbf{y}_i^s$. Then after averaging, the effect of the concealing samples would not be ignored. The gradient contains the information about the sensitive data, the concealing sample obfuscates the gradient, so the reconstruction through such gradient would also contain the information from the concealing sample, which could visually obfuscate the reversed sensitive data.

In general, we need to satisfy three goals as part of our defence:

- **Goal-1:** To imitate the sensitive data point, the concealing sample should have high gradient similarity with the sensitive data point.
- **Goal-2:** To protect the sensitive information, the reconstructed data through the new gradients should be visually dissimilar from the sensitive data.
- **Goal-3:** To maintain the performance of the model, the new gradient direction should be similar to the original gradient direction.

We now propose our formulation to achieve these three goals. To simplify the formulation, but without loss of generality, we assume one client here. Suppose the mini-batch contains data points $\mathbf{X} = \{\mathbf{x}_1, \mathbf{x}_2, \dots, \mathbf{x}_n\} \in \mathbb{R}^{n \times d}$ and m data points are sensitive ones $\mathbf{X}_s = \{\mathbf{x}_{n-m+1}, \dots, \mathbf{x}_n\} \in \mathbb{R}^{m \times d}$. For simplicity, we craft the concealing samples start from data points $\mathbf{X}_r = \{\mathbf{x}_{n-m-(r+1)k+1}, \dots, \mathbf{x}_{n-m-rk}\} \in \mathbb{R}^{k \times d}$ for each sensitive data point $\mathbf{x}_{n-r} \in \mathbf{X}_s$, where $k \geq 1$ decides how many concealing samples would be inserted for the sensitive data \mathbf{x}_{n-r} with $r \in [0, m-1]$ and $n \geq m(k+1)$. We also include the setting where crafting concealing samples start from random noise and data from other dataset in Section 4. Therefore, we get a new mini-batch $\tilde{\mathbf{X}}$ as the input, the concealing samples $\tilde{\mathbf{X}}_r$ will satisfy $\forall \tilde{\mathbf{x}}_i \in \tilde{\mathbf{X}}_r$ ($i \in [1, k]$),

$$\begin{aligned} & \max_{\tilde{\mathbf{x}}_i} \quad \|\tilde{\mathbf{x}}_i - \mathbf{x}_{n-r}\|, \\ & \min_{\tilde{\mathbf{x}}_i} \quad \|\nabla_{\theta}\mathcal{L}(f_{\theta}(\tilde{\mathbf{x}}_i), \mathbf{y}_i) - \nabla_{\theta}\mathcal{L}(f_{\theta}(\mathbf{x}_{n-r}), \mathbf{y}_{n-r})\|, \\ & s.t. \quad \langle \nabla_{\theta}\mathcal{L}(f_{\theta}(\tilde{\mathbf{X}}), \mathbf{Y}), \nabla_{\theta}\mathcal{L}(f_{\theta}(\mathbf{X}), \mathbf{Y}) \rangle \geq 0. \end{aligned} \quad (6)$$

The first formulation in Eqn. (6) aims to meet Goal-2, letting the concealing sample $\tilde{\mathbf{x}}_i$ is visually dissimilar from the sensitive data point \mathbf{x}_{n-r} , while the second one aims to meet Goal-1, letting the concealing sample imitate the sensitive data point in the gradient level. As such, the adversaries aiming to reconstruct the sensitive data points will be confused by the concealing samples. To achieve Goal-3, we adopt the constraints to make sure the direction of the gradient over the new mini-batch is align to that over the original mini-batch, trying to avoid significant drop on the model performance after inserting the concealing samples. In addition, to increase the defence ability against the Imprint attack (Fowl *et al.*, 2021) which only need the data point to activate one line in the weights alone, we add an extra constraint aiming to let the distance between the latent features extracted from the concealing samples and the sensitive data points is bounded: $\|h_{\theta}(\tilde{\mathbf{x}}_i) - h_{\theta}(\mathbf{x}_{n-r})\| \leq \epsilon$, where h_{θ} denotes the latent feature extractor and ϵ controls the latent feature distance between the concealing data and the sensitive data. As such, reduce the possibility of one data point activate one line alone.

Further, since the gradient of the concealing samples is similar to that of the sensitive data point, which means the concealing sample already have the same part information from the sensitive data point contributing to the model decision, we can try to dismiss the gradient of the sensitive data without compromising on their contribution towards training the model to provide a stronger protection. To achieve this, the constraints in Eqn. (6) could be rewritten as:

$$\langle \nabla_{\theta}\mathcal{L}(f_{\theta}(\tilde{\mathbf{X}}), \mathbf{Y}), \nabla_{\theta}\mathcal{L}(f_{\theta}(\mathbf{X} \setminus \mathbf{X}_s), \mathbf{Y} \setminus \mathbf{Y}_s) \rangle \geq 0, \quad (7)$$

where $\mathbf{X} \setminus \mathbf{X}_s$ denotes data points in the mini-batch excluding the sensitive data points.

We now provide a solution for Eqn. (6) to obtain such concealing samples by defining an objective function \mathcal{L}_{obj} as follows:

$$\begin{aligned} \mathcal{L}_{obj} = & \sum_{r=0}^{m-1} \sum_{i=1}^k \left(1 - \frac{\langle \nabla_{\theta} \mathcal{L}(f_{\theta}(\tilde{\mathbf{x}}_i), \mathbf{y}_i), \nabla_{\theta} \mathcal{L}(f_{\theta}(\mathbf{x}_{n-r}), \mathbf{y}_{n-r}) \rangle}{\|\nabla_{\theta} \mathcal{L}(f_{\theta}(\tilde{\mathbf{x}}_i), \mathbf{y}_i)\| \times \|\nabla_{\theta} \mathcal{L}(f_{\theta}(\mathbf{x}_{n-r}), \mathbf{y}_{n-r})\|} \right. \\ & \left. + \frac{\alpha}{\|\tilde{\mathbf{x}}_i - \mathbf{x}_{n-r}\|} + \beta \|h_{\theta}(\tilde{\mathbf{x}}_i) - h_{\theta}(\mathbf{x}_{n-r})\| \right), \end{aligned} \quad (8)$$

where α and β are hyper-parameters to determine how much the focus would be on the distance between the concealing samples and the sensitive data points, and the distance between the latent features from the concealing samples and those from the sensitive data points. In Eqn. (8), the first term is for achieving Goal-1 that makes the concealing samples are similar to the sensitive data points in the gradient level, the second term is for achieving Goal-2 that makes the concealing samples are visually dissimilar to the sensitive data points, while the last term aims to avoid one data point activate one row in the weights alone.

We apply Adam optimizer (Kingma and Ba, 2015) to solve Eqn. (8) for generating the concealing samples. The concealing samples are computed starting from the data points sampled from the dataset or random noise. Considering the concealing samples have high gradient and latent feature similarity with the sensitive data points, which means features from the concealing samples contain both information from the sensitive data points and that from the concealing samples, the concealing samples would have high chance to be near the decision boundary if the start points are data points having different label with the sensitive data point. In this case, to ensure the concealing samples does not degrade the model performance significantly, we employ the loss mixup (Zhang *et al.*, 2017) to compute the new gradients. Supposing all the concealing samples $\tilde{\mathbf{X}}_r (r \in [0, m-1])$ for the sensitive data point \mathbf{x}_{n-r} are represented as $\tilde{\mathbf{X}}_c$, the new gradients from the new mini-batch $\tilde{\mathbf{X}}$ are computed as follows:

$$\begin{aligned} \nabla_{\theta} \mathcal{L}(f_{\theta}(\tilde{\mathbf{X}}, \mathbf{Y})) = & \nabla_{\theta} (\lambda \mathcal{L}(f_{\theta}(\tilde{\mathbf{X}}_c), \mathbf{Y}_c) + (1 - \lambda) \mathcal{L}(f_{\theta}(\tilde{\mathbf{X}}_c), \mathbf{Y}_{sen}) \\ & + \mathcal{L}(f_{\theta}(\tilde{\mathbf{X}} \setminus \tilde{\mathbf{X}}_c), \mathbf{Y} \setminus \mathbf{Y}_c)), \end{aligned} \quad (9)$$

where $0 < \lambda < 1$. Inspired by the technique proposed in Lopez-Paz and Ranzato (2017) to avoid forgetting in continual learning, we perform the gradient projection on the new gradients using Eqn. (7) to further ensure that the new mini-batch would not significantly degrade the model performance.

4 Experiments

In this section, we present the experimental results of the proposed defence method. We first demonstrate the settings, compare the defence performance with other defences against model inversion attacks in Federated Learning (FL). Then, we evaluate the FL performance with defence techniques on Independent and Identically Distributed (IID) and Not Independent and Identically Distributed (Non-IID) settings. Also, we show the performance when combining the proposed defence and other defences for adaptive protections. Further, we analyze the proposed defence method with different start points for computing the concealing samples.

4.1 Experimental setup

Here, we give the overall settings and details can be found in the Appendix A.

Attack methods We follow the recent study (Balunović *et al.*, 2021) to evaluate defences against two optimization-based attacks in FL: the classical optimization-based method named *DLG attack* (Zhu *et al.*, 2019), an improved version called *GS attack* (Geiping *et al.*, 2020) that introduces image prior and uses cosine similarity as distance metric. We also include one model modification attack: the recently proposed *Imprint attack* (Fowl *et al.*, 2021).

Defence baselines We follow the recent study (Sun *et al.*, 2021) to compare with existing defences including traditional defences *DP* (Differential Privacy) (McMahan *et al.*, 2017b) and *Prune* (Gradient

Table 1: Performance of defences against model inversion attacks.

Defence	DLG		GS		Imprint		Imprint	
	PSNR↓	SSIM↓	PSNR↓	SSIM↓	PSNR↓	SSIM↓	PSNR↓	SSIM↓
<i>MNIST</i>						<i>HAM10000</i>		
-	31.95	0.75	45.25	0.92	82.43	1.0	119.69	0.99
Prune	9.56	0.24	11.69	0.28	75.41	0.96	48.86	0.86
Gaussian	19.51	0.44	22.83	0.51	53.87	0.99	53.56	0.97
Laplacian	16.17	0.38	19.45	0.44	51.35	0.99	51.73	0.97
Soteria	11.69	0.29	11.48	0.22	82.43	1.0	-	-
Ours	5.98	0.12	10.58	0.22	19.95	0.60	20.28	0.83
<i>CIFAR10</i>						<i>CelebA</i>		
-	15.85	0.52	18.50	0.65	140.62	0.98	154.79	1.0
Prune	13.37	0.35	10.67	0.22	15.44	0.54	29.54	0.70
Gaussian	8.14	0.12	8.73	0.14	33.21	0.86	64.60	0.95
Laplacian	7.57	0.10	7.97	0.12	32.18	0.85	62.12	0.95
Soteria	12.22	0.33	9.08	0.14	140.62	0.98	-	-
Ours	5.49	0.08	6.39	0.11	14.14	0.49	15.85	0.64

Compression) (Lin *et al.*, 2017), and we also include the recently proposed defence *Soteria* (Sun *et al.*, 2021). In the paper, we do not consider the defences which alter the sensitive data or modify the models architectures. But in the appendix, we show the comparison with such defences like PRE-CODE (PRivacy EnhanCing mODulE) (Scheliga *et al.*, 2022) and ATS (Automatic Transformation Search) (Gao *et al.*, 2021).

Datasets We evaluate defences on four datasets, namely MNIST (LeCun *et al.*, 1998), CIFAR10 (Krizhevsky *et al.*, 2009), a medical dataset HAM10000 (Tschandl *et al.*, 2018) and CelebFaces Attributes Dataset CelebA (Liu *et al.*, 2015).

Models We consider three model architectures with different complexities. LeNet (LeCun *et al.*, 1998) for the MNIST dataset, which has four convolutional layers and one fully connected layer, and uses Sigmoid as non-linear activation function. ConvNet for CIFAR10 dataset having the same model structure that was used in *Soteria* (Sun *et al.*, 2021) where activation layers are ReLU. We use the ResNet18 (He *et al.*, 2016) for HAM10000 and CelebA datasets.

Evaluation metrics To compare between the sensitive data and their reconstructions, we use peak signal-to-noise ratio (PSNR) as used in the paper (Balunović *et al.*, 2021) and structural similarity index measure (SSIM) (Wang *et al.*, 2004). For PSNR and SSIM, the smaller the number, the better the performance. We use accuracy on the test set to measure overall models performance. We use balanced accuracy on the CelebA dataset.

4.2 Defence results

The ideal conditions for the adversaries to invert gradients are the batch size is small and the target network is not yet trained. So we evaluate on non-trained networks whose weights are randomly initialized for MNIST, CIFAR10 and HAM10000, while evaluate on the pre-trained model for CelebA. We consider the batch size as 2 for the DLG and GS attack methods, and consider the batch size as 4 for the Imprint attack. We suppose that each batch has one sensitive data point. Our defence method therefore learns one concealing sample in the mini-batch.

On MNIST, for the DLG and GS attacks, we randomly select 273 images (we set 100 clients and randomly assign the train set to each client, then select one client to test). For the Imprint attack, we randomly select 64 images (different batches from the sub train set of the client). As shown in Table 1, when defending against the model inversion attacks, compared with other defences, our method provides the best protection. Specifically, against the DLG attack, the defence baselines reduce the PSNR from 31.95 to about 10, while our defence method can reduce the PSNR to less

Table 2: FL performance without and with defences.

Defence	MNIST		CIFAR10		HAM10000		CelebA	
	IID \uparrow	Non-IID \uparrow	IID \uparrow	Non-IID \uparrow	IID \uparrow	Non-IID \uparrow	IID \uparrow	Non-IID \uparrow
-	92.08	68.03	73.55	42.02	85.31	74.07	85.34	81.59
Prune	91.31	66.26	67.55	38.30	83.50	70.81	86.14	83.65
Gaussian	91.91	67.99	67.08	37.83	82.96	71.08	84.91	83.92
Laplacian	91.95	67.80	66.67	39.7	82.86	70.63	82.63	83.54
Soteria	92.06	68.05	66.91	38.04	-	-	-	-
Ours	93.12	72.46	68.86	41.23	83.59	71.80	86.80	84.48

than 6. When defending against the Imprint attack, the defence Soteria cannot know where and when the adversary would insert the imprint module, so it cannot withstand the Imprint attack. Also, our method reduces the SSIM to 0.6 when other defences only reduce it to around 0.96.

On CIFAR10, we apply the same strategy as that on MNIST to sample images. The number of images for testing the DLG and GS attack is 227. As shown in Table 1, our defence method achieves the least PSNR and SSIM, which means we provide the best protection.

Further, we evaluate defences on a medical dataset HAM10000 and a face attributes dataset CelebA where images have large resolutions. Because the reconstructions of the DLG and GS attacks does not perform well on these dataset, so we only test defences against the Imprint attack. For CelebA dataset, we use the attribute *smiling* as the target label to perform binary classification. As shown in Table 1, our defence method still has the best protection on these dataset.

4.3 Utility

While we have already showed that our defence provide the best protection, the FL utility is significant and we now show the performance with defences (we use the same hyper parameters for all methods used in Table 1). On the IID setting, the server randomly select 5 from 10 clients in each round. On the Non-IID setting, the server updates the model using gradients from the 10 clients. All methods have same number of training examples. We first show how these defences perform when the proportion of sensitive data is very small.

On MNIST, each client has 2000 samples randomly sampled from the train set on the IID setting, while on the Non-IID setting, each client only has 400 samples with 2 labels, each label has 200 samples. The performance is evaluated on 10,000 test images. As shown in Table 2, when other defences cause performance drop, our defence retains the performance and even enhances it in some cases, thanks to our matching gradient projections.

On CIFAR10, we also apply the same mechanism as that for MNIST to train the FL framework. The difference is, on the Non-IID setting, each client has 4000 samples with 2 labels, and each label has 2000 samples. As shown in Table 2, our defence method cause the least drop in the performance. Specifically, when the defence baseline drop the performance by about 4%, our defence largely retains the performance and only shows a drop by less than 1% on the Non-IID setting.

On HAM10000, we randomly select 200 images for each client on the IID setting. On the Non-IID setting, each client has images sampled from 2 labels. The server tests on 1103 images and trains for 100 rounds. As shown in Table 2, our defence method still has the best protection while keeping the FL performance. Same results also shown on CelebA.

In summary, we can conclude that compared with other defences, our method has the best protection. When the proportion of sensitive data points is small, our defence can also maintain the FL performance. In this case, it is not necessary to use defence like gradient compression which would protect all data but have a significantly drop the model performance.

4.4 Combination Results

Given that different data points may need different attentions, we could combine our defence with existing defence to provide different protection for different data points, as such, the final combined

Table 3: Combination of defences. PSNR and SSIM are computed between all the sensitive images.





Defence	GS		Example	Accuracy	
	PSNR↓	SSIM↓		IID↑	Non-IID↑
-	25.16	0.64		92.08	68.03
Gaussian (1e-3)	24.69	0.63		92.07	68.00
Gaussian (1e-2)	13.64	0.31		91.91	67.99
Ours_Gaussian (1e-3)	12.74	0.26		93.12	72.47

Table 4: Different start point for crafting the concealing samples.

Start point	DLG		GS		Imprint		Accuracy	
	PSNR↓	SSIM↓	PSNR↓	SSIM↓	PSNR↓	SSIM↓	IID↑	Non-IID↑
MNIST	6.00	0.12	10.58	0.22	19.95	0.60	93.11	72.52
QMIST	6.04	0.13	10.86	0.23	14.68	0.57	93.05	72.50
Noise	5.66	0.12	10.03	0.19	18.68	0.35	93.13	72.43

technique can provide best protection while keeping the model performance for all data points in different cases. We craft one concealing sample for one sensitive data, and then adopt DP to add Gaussian noise into the gradients. As shown in Table 3, the combined technique could provide the best protection for all data points while achieving the best model performance. When we only combine our defence and DP, we only craft one concealing sample for the data point ‘6’, and add noise whose scale is 0.001, the combined defence can provide the same protection as that noise whose scale is 0.01, while the latter could drop the model performance.

4.5 Start point for crafting the concealing samples

We show the results when crafting the concealing samples using different start points. As shown in Table 4, even start from random noise, our defence method could still provide protection and keep the model performance. In fact, if the start point has more different distribution with the sensitive data points, the proposed defence technique could be more effective. Examples can be found in the Appendix A.

4.6 Discussion and future work

Our experimental evaluation show the effective of the proposed defence. However, it requires additional compute to generate concealing samples, and has restriction on proportion of sensitive samples within a mini-batch, while we could combine other defence with our method to overcome this problem. Besides, unlike defences such as differential privacy and gradient compression, our defence method cannot be applied to tasks like natural language processing. Future directions to improve concealing samples based defence include the design of few or even no hyper parameters, finding the best starting points and reducing the time to compute the concealing samples. We hope our defence could provide a new perspective for defending against model inversion attacks in FL.

5 Conclusion

In this work, we proposed a practical and effective defence against model inversion attacks in FL. We introduced concealing samples that imitate the sensitive data, but can obfuscate the gradients of the sensitive data. Our proposed approach ensures that the concealing samples is visually dissimilar to the sensitive data, thus aiming to obfuscate the constructed sensitive information. Our proposed concealing samples are adaptively learned to provide protection for the sensitive data and simultaneously avoid performance drop. Experiments showed that, compared with other defences, our approach offers the best protection against model inversion attacks without sacrificing the FL performance.

References

- Mislav Balunović, Dimitar I Dimitrov, Robin Staab, and Martin Vechev. Bayesian framework for gradient leakage. *arXiv preprint arXiv:2111.04706*, 2021.
- Daniel J Beutel, Taner Topal, Akhil Mathur, Xinchu Qiu, Titouan Parcollet, and Nicholas D Lane. Flower: A friendly federated learning research framework. *arXiv preprint arXiv:2007.14390*, 2020.
- Franziska Boenisch, Adam Dziedzic, Roei Schuster, Ali Shahin Shamsabadi, Ilia Shumailov, and Nicolas Papernot. When the curious abandon honesty: Federated learning is not private. *arXiv preprint arXiv:2112.02918*, 2021.
- Keith Bonawitz, Vladimir Ivanov, Ben Kreuter, Antonio Marcedone, H Brendan McMahan, Sarvar Patel, Daniel Ramage, Aaron Segal, and Karn Seth. Practical secure aggregation for privacy-preserving machine learning. In *proceedings of the 2017 ACM SIGSAC Conference on Computer and Communications Security*, pages 1175–1191, 2017.
- Theodora S Brisimi, Ruidi Chen, Theofanie Mela, Alex Olshevsky, Ioannis Ch Paschalidis, and Wei Shi. Federated learning of predictive models from federated electronic health records. *International journal of medical informatics*, 112:59–67, 2018.
- Nicholas Carlini, Samuel Deng, Sanjam Garg, Somesh Jha, Saeed Mahloujifar, Mohammad Mahmoody, Shuang Song, Abhradeep Thakurta, and Florian Tramèr. Is private learning possible with instance encoding? *arXiv preprint arXiv:2011.05315*, 2020.
- Jia Deng, Wei Dong, Richard Socher, Li-Jia Li, Kai Li, and Li Fei-Fei. Imagenet: A large-scale hierarchical image database. In *2009 IEEE conference on computer vision and pattern recognition*, pages 248–255. Ieee, 2009.
- Lixin Fan, Kam Woh Ng, Ce Ju, Tianyu Zhang, Chang Liu, Chee Seng Chan, and Qiang Yang. Rethinking privacy preserving deep learning: How to evaluate and thwart privacy attacks. In *Federated Learning*, pages 32–50. Springer, 2020.
- Liam Fowl, Jonas Geiping, Wojtek Czaja, Micah Goldblum, and Tom Goldstein. Robbing the fed: Directly obtaining private data in federated learning with modified models. *arXiv preprint arXiv:2110.13057*, 2021.
- Wei Gao, Shangwei Guo, Tianwei Zhang, Han Qiu, Yonggang Wen, and Yang Liu. Privacy-preserving collaborative learning with automatic transformation search. In *Proceedings of the IEEE/CVF Conference on Computer Vision and Pattern Recognition*, pages 114–123, 2021.
- Jonas Geiping, Hartmut Bauermeister, Hannah Dröge, and Michael Moeller. Inverting gradients-how easy is it to break privacy in federated learning? *Advances in Neural Information Processing Systems*, 33:16937–16947, 2020.
- Robin C Geyer, Tassilo Klein, and Moin Nabi. Differentially private federated learning: A client level perspective. *arXiv preprint arXiv:1712.07557*, 2017.
- Oded Goldreich. *Foundations of cryptography: volume 2, basic applications*. Cambridge university press, 2009.
- Kaiming He, Xiangyu Zhang, Shaoqing Ren, and Jian Sun. Deep residual learning for image recognition. In *Proceedings of the IEEE conference on computer vision and pattern recognition*, pages 770–778, 2016.
- Yangsibo Huang, Zhao Song, Kai Li, and Sanjeev Arora. Instahide: Instance-hiding schemes for private distributed learning. In *International Conference on Machine Learning*, pages 4507–4518. PMLR, 2020.
- Yangsibo Huang, Samyak Gupta, Zhao Song, Kai Li, and Sanjeev Arora. Evaluating gradient inversion attacks and defenses in federated learning. *Advances in Neural Information Processing Systems*, 34, 2021.
- Jinwoo Jeon, Kangwook Lee, Sewoong Oh, Jungseul Ok, et al. Gradient inversion with generative image prior. *Advances in Neural Information Processing Systems*, 34:29898–29908, 2021.
- Xiao Jin, Pin-Yu Chen, Chia-Yi Hsu, Chia-Mu Yu, and Tianyi Chen. Catastrophic data leakage in vertical federated learning. *Advances in Neural Information Processing Systems*, 34, 2021.
- Peter Kairouz, H Brendan McMahan, Brendan Avent, Aurélien Bellet, Mehdi Bennis, Arjun Nitin Bhagoji, Kallista Bonawitz, Zachary Charles, Graham Cormode, Rachel Cummings, et al. Advances and open problems in federated learning. *Foundations and Trends® in Machine Learning*, 14(1–2):1–210, 2021.
- Diederik P Kingma and Jimmy Ba. Adam: A method for stochastic optimization. In *ICLR (Poster)*, 2015.

- Jakub Konečný, Brendan McMahan, and Daniel Ramage. Federated optimization: Distributed optimization beyond the datacenter. *arXiv preprint arXiv:1511.03575*, 2015.
- Alex Krizhevsky, Geoffrey Hinton, et al. Learning multiple layers of features from tiny images. 2009.
- Yann LeCun, Léon Bottou, Yoshua Bengio, and Patrick Haffner. Gradient-based learning applied to document recognition. *Proceedings of the IEEE*, 86(11):2278–2324, 1998.
- Hongkyu Lee, Jeehyeong Kim, Seyoung Ahn, Rasheed Hussain, Sunghyun Cho, and Junggab Son. Digestive neural networks: A novel defense strategy against inference attacks in federated learning. *computers & security*, 109:102378, 2021.
- Yujun Lin, Song Han, Huizi Mao, Yu Wang, and William J Dally. Deep gradient compression: Reducing the communication bandwidth for distributed training. *arXiv preprint arXiv:1712.01887*, 2017.
- Ziwei Liu, Ping Luo, Xiaogang Wang, and Xiaoou Tang. Deep learning face attributes in the wild. In *Proceedings of International Conference on Computer Vision (ICCV)*, December 2015.
- David Lopez-Paz and Marc’ Aurelio Ranzato. Gradient episodic memory for continual learning. *Advances in neural information processing systems*, 30, 2017.
- Brendan McMahan, Eider Moore, Daniel Ramage, Seth Hampson, and Blaise Aguera y Arcas. Communication-efficient learning of deep networks from decentralized data. In *Artificial intelligence and statistics*, pages 1273–1282. PMLR, 2017.
- H Brendan McMahan, Daniel Ramage, Kunal Talwar, and Li Zhang. Learning differentially private recurrent language models. *arXiv preprint arXiv:1710.06963*, 2017.
- Fan Mo, Anastasia Borovykh, Mohammad Malekzadeh, Hamed Haddadi, and Soteris Demetriou. Quantifying information leakage from gradients. *CoRR, abs/2105.13929*, 2021.
- Payman Mohassel and Yupeng Zhang. Secureml: A system for scalable privacy-preserving machine learning. In *2017 IEEE symposium on security and privacy (SP)*, pages 19–38. IEEE, 2017.
- Le Trieu Phong, Yoshinori Aono, Takuya Hayashi, Lihua Wang, and Shiho Moriai. Privacy-preserving deep learning: Revisited and enhanced. In *International Conference on Applications and Techniques in Information Security*, pages 100–110. Springer, 2017.
- Daniel Scheliga, Patrick Mäder, and Marco Seeland. Precode-a generic model extension to prevent deep gradient leakage. In *Proceedings of the IEEE/CVF Winter Conference on Applications of Computer Vision*, pages 1849–1858, 2022.
- Jingwei Sun, Ang Li, Binghui Wang, Huanrui Yang, Hai Li, and Yiran Chen. Soteria: Provable defense against privacy leakage in federated learning from representation perspective. In *Proceedings of the IEEE/CVF Conference on Computer Vision and Pattern Recognition*, pages 9311–9319, 2021.
- Philipp Tschandl, Cliff Rosendahl, and Harald Kittler. The ham10000 dataset, a large collection of multi-source dermatoscopic images of common pigmented skin lesions. *Scientific data*, 5(1):1–9, 2018.
- Zhou Wang, Alan C Bovik, Hamid R Sheikh, and Eero P Simoncelli. Image quality assessment: from error visibility to structural similarity. *IEEE transactions on image processing*, 13(4):600–612, 2004.
- Wenqi Wei, Ling Liu, Margaret Loper, Ka-Ho Chow, Mehmet Emre Gursoy, Stacey Truex, and Yanzhao Wu. A framework for evaluating client privacy leakages in federated learning. In *European Symposium on Research in Computer Security*, pages 545–566. Springer, 2020.
- Wenqi Wei, Ling Liu, Yanzhao Wut, Gong Su, and Arun Iyengar. Gradient-leakage resilient federated learning. In *2021 IEEE 41st International Conference on Distributed Computing Systems (ICDCS)*, pages 797–807. IEEE, 2021.
- Hongxu Yin, Arun Mallya, Arash Vahdat, Jose M Alvarez, Jan Kautz, and Pavlo Molchanov. See through gradients: Image batch recovery via gradinversion. In *Proceedings of the IEEE/CVF Conference on Computer Vision and Pattern Recognition*, pages 16337–16346, 2021.
- Hongyi Zhang, Moustapha Cisse, Yann N Dauphin, and David Lopez-Paz. mixup: Beyond empirical risk minimization. *arXiv preprint arXiv:1710.09412*, 2017.
- Richard Zhang, Phillip Isola, Alexei A Efros, Eli Shechtman, and Oliver Wang. The unreasonable effectiveness of deep features as a perceptual metric. In *CVPR*, 2018.

Bo Zhao, Konda Reddy Mopuri, and Hakan Bilen. idlg: Improved deep leakage from gradients. *arXiv preprint arXiv:2001.02610*, 2020.

Ligeng Zhu, Zhijian Liu, and Song Han. Deep leakage from gradients. *Advances in Neural Information Processing Systems*, 32, 2019.

A Appendix

Here we provide additional details.

A.1 Compared with PRECODE and ATS

Table 5: Compared with PRECODE and ATS on CIFAR10.

Defence	GS		Imprint		Accuracy	
	PSNR↓	SSIM↓	PSNR↓	SSIM↓	IID↑	Non-IID↑
PRECODE	5.06	0.07	120.02	0.85	67.06	28.44
ATS	17.50	0.47	49.97	0.48	60.46	37.89
Ours	6.43	0.11	14.14	0.49	68.05	41.86

A.2 Examples of different start point

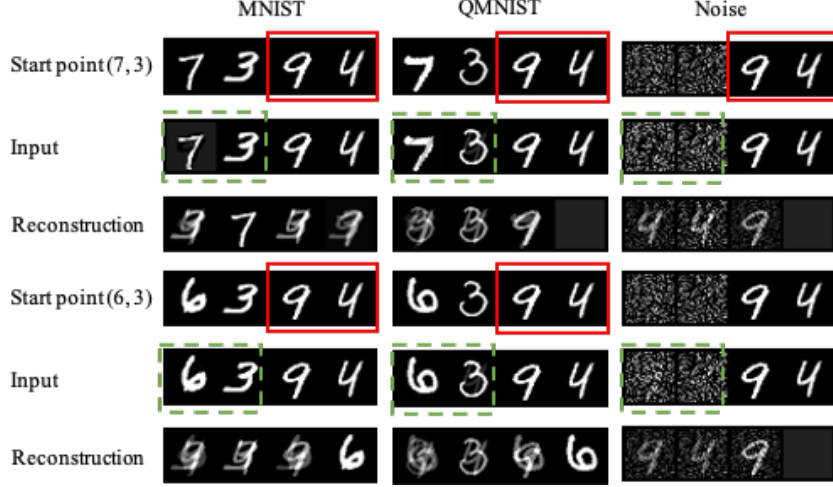


Figure 1: Examples of reconstruction for defences against the Imprint attack on MNIST when using different start point to craft the camouflage data. Images in the red solid box and green dashed box are the sensitive data and the camouflage data, respectively.

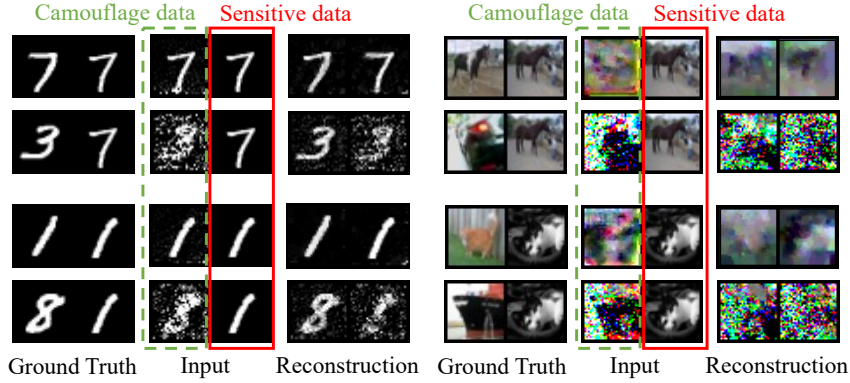


Figure 2: Examples of the reconstruction for the situations where camouflage data are computed from data with the same or different labels as the sensitive data. Images in the red solid box and green dashed box are the sensitive data and the camouflage data, respectively.

A.3 Examples of reconstructions

Figure 3 and Figure 4 show the examples of reconstructions. Figure 3 and Figure 4 (a) show the reconstructions after applying different defences against the Imprint attack and GS attack, respectively. Our defence method could effectively hide the sensitive data with the camouflage data.

Results on ImageNet Further, we evaluate our defence method on the dataset ImageNet (Deng *et al.*, 2009). As shown in Figure 4 (b), when our defence method uses more camouflage data points to imitate the sensitive data point, the performance of defence against the Imprint attacks is better, which is aligned with the results when defending against the GS attack shown in Table ?? . Besides, we also evaluate our defence method on 66 images randomly sampled from the validation set of ImageNet against the GS attack. We consider the batch size as 2. Without any defences, the metric PSNR, SSIM and LPIPS (Zhang *et al.*, 2018) is 12.51, 0.12 and 0.71, respectively. When applying our defence method, the metric PSNR, SSIM and LPIPS is 6.81, 0.02 and 0.94, respectively. Notice that when the value of PSNR and SSIM is smaller and the value of LPIPS is larger, the defence

performance is better. We can conclude that our defence method also provide an effective protection for the sensitive data on the ImageNet dataset against the model inversion attacks in FL.

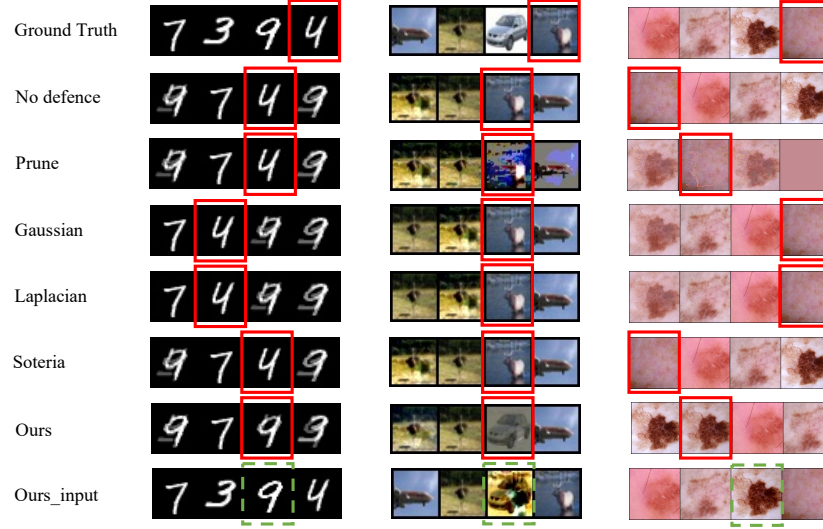


Figure 3: Examples of reconstruction for defences against the Imprint attack on MNIST, CIFAR10 and HAM10000, respectively. The parameters for defences are the same as those in Table ?? and Table ?. Images in red solid box are sensitive data points and their reconstructions. Images in green dashed box are camouflage data points in our defence method.

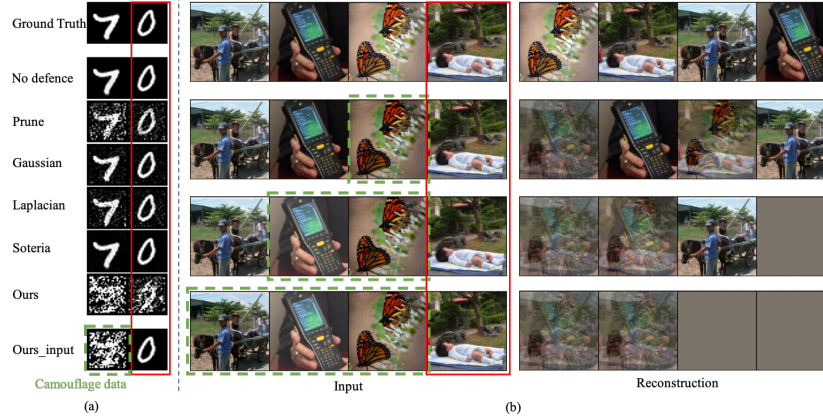


Figure 4: (a) Examples of reconstruction for defences against the GS attack on MNIST. (b) Examples of reconstruction for our defence against the Imprint Attack on ImageNet. Images in read solid box are sensitive data and their reconstructions. Images in green dashed box are camouflage data points.

A.4 Model Architectures

Details of the models used in this study are shown in Table 6. The activation layers of the model for MNIST are Sigmoid, and for CIFAR10 and HAM10000, CelebA are ReLU.

Table 6: Model architectures for different datasets.

MNIST	CIFAR10	HAM10000 / CelebA
5×5 Conv, 12	5×5 Conv, 32	7×7 Conv, 64
5×5 Conv, 12	$\{5 \times 5$ Conv, 64 $\} \times 2$	3×3 MaxPool
5×5 Conv, 12	$\{5 \times 5$ Conv, 128 $\} \times 3$	$\left\{ \begin{array}{l} 3 \times 3 \text{ Conv, 64} \\ 3 \times 3 \text{ Conv, 64} \end{array} \right\} \times 2$
5×5 Conv, 12	3×3 MaxPool	$\left\{ \begin{array}{l} 3 \times 3 \text{ Conv, 128} \\ 3 \times 3 \text{ Conv, 128} \end{array} \right\} \times 2$
FC-10	$\{5 \times 5$ Conv, 128 $\} \times 3$	$\left\{ \begin{array}{l} 3 \times 3 \text{ Conv, 256} \\ 3 \times 3 \text{ Conv, 256} \end{array} \right\} \times 2$
	3×3 MaxPool	$\left\{ \begin{array}{l} 3 \times 3 \text{ Conv, 512} \\ 3 \times 3 \text{ Conv, 512} \end{array} \right\} \times 2$
	FC-10	7×7 AveragePool
		FC-7

A.5 Parameters

Model inversion attack Details of parameters of different defences against model inversion attacks are shown in Table 7. The per cent number of pruning for the defence Prune and the defence Soteria is denoted as p . The standard deviation $\sigma = 0$ for DP adding Gaussian or Laplacian noise, with variance denoted as $scale$.

We built on the repository using the official implementation of the DLG and GS attacks, the Imprint attack (which is licensed under MIT License) and the defence Soteria.

Table 7: Parameters of different defences against model inversion attacks.

Dataset	Defence	DLG and GS attacks	Imprint attack
MNIST	Prune	$p = 70\%$	$p = 30\%$
	Gaussian	$scale = 1e - 2$	$scale = 1e - 2$
	Laplacian	$scale = 1e - 2$	$scale = 1e - 2$
	Soteria	$p = 5\%, p = 1\%$	$p = 1\%$
	Ours	$\alpha = 0.1, \beta = 0.001$ $T = 1000, \lambda = 0.3$	$\alpha = 30., \beta = 100.$ $T = 100, \lambda = 0.3$
CIFAR10	Prune	$p = 70\%$	$p = 70\%$
	Gaussian	$scale = 1e - 3$	$scale = 1e - 3$
	Laplacian	$scale = 1e - 3$	$scale = 1e - 3$
	Soteria	$p = 90\%$	$p = 90\%$
	Ours	$\alpha = 0.1, \beta = 0.001$ $T = 1000, \lambda = 0.3$	$\alpha = 30., \beta = 100.$ $T = 100, \lambda = 0.3$
HAM10000	Prune	-	$p = 50\%$
	Gaussian	-	$scale = 1e - 1$
	Laplacian	-	$scale = 1e - 1$
	Ours	-	$\alpha = 30., \beta = 100.$ $T = 100, \lambda = 0.3$

Federated learning (FL) We build the FL framework based on the Flower (Beutel *et al.*, 2020) platform and the FedAvg (McMahan *et al.*, 2017a) algorithm. The details of the federated learning are shown in Table 8. For the Independent and Identically Distributed (IID) setting, the server randomly

Table 8: Details of the federated learning on different dataset. Training samples and Labels denote the number of training data and the number of labels in each client, respectively.

Dataset	Training samples	Labels	Batch size	Learning rate	Training rounds
<i>on the IID setting</i>					
MNIST	2,000	10	256	0.01	100
CIFAR10	2,000	10	256	0.01	100
HAM10000	200	7	32	0.001	100
<i>on the Non-IID setting</i>					
MNIST	400	2	256	0.01	100
CIFAR10	4,000	2	256	0.001	100
HAM10000	214~958	2	32	0.0001	100

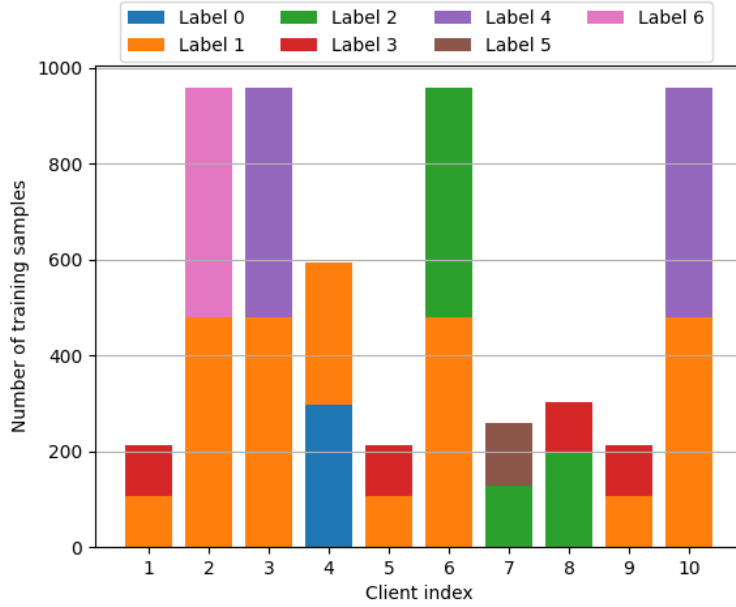


Figure 5: The distribution of training samples from HAM10000 on clients on the Non-IID setting.

selects five from 10 clients in each round. Each client has 2000 samples for MNIST and CIFAR10, 200 samples for HAM10000 randomly sampled from the train set. For the Not Independent and Identically Distributed (Non-IID) setting, the server updates the model using gradients from the ten clients. Each client only has 400 samples for MNIST, and 4000 samples for CIFAR10 with two labels. Each label has 200 samples for MNIST, and 2000 samples for CIFAR10. For HAM10000, as shown in Figure 5, each client has 214, 958, 958, 594, 214, 958, 258, 214, 214, 958 samples, respectively in the Non-IID setting. The performance is evaluated on 10,000, 10,000 and 1103 test samples for MNIST, CIFAR10 and HAM10000, respectively. The optimizer is SGD, and the batch size is 256 for MNIST and CIFAR10, 32 for HAM10000 for each client, and the maximum number of training rounds is 100.